JOM

A publication of The Minerals, Metals & Materials Society

FEBRUARY 1998

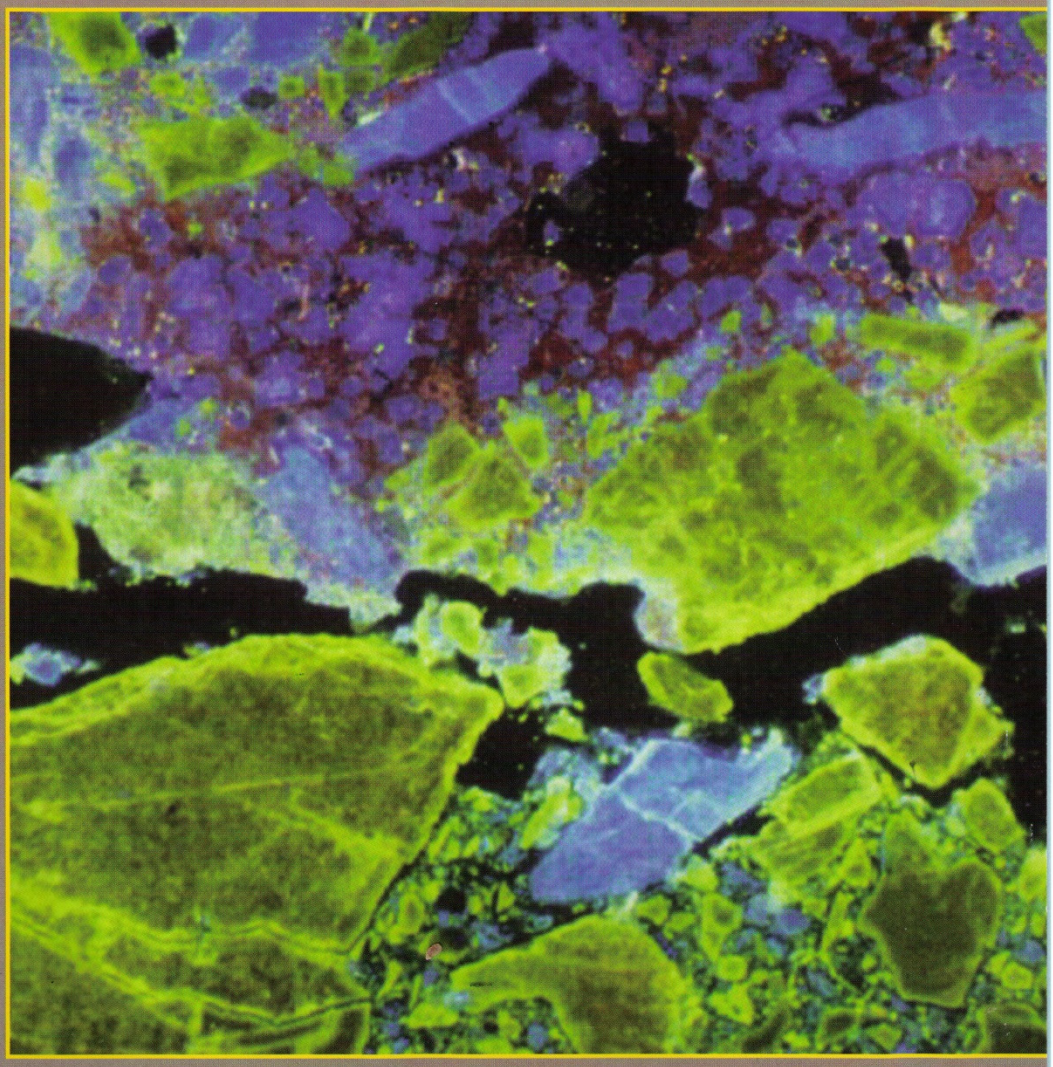

- **Aluminum Production: Molten Metal Effects**
- **Opportunities in Grain Boundary Engineering**

Also in this issue
JOM-e: Electromagnetic Fields and Solidification;
1998 TMS Honors and Awards

The Mineralogical Characterization of Dry-Powder Barriers in Al Reduction Cells

Ann M. Hagni

Dry-powder barrier layers have been investigated in recent years to prevent fluorine penetration and degradation of insulating refractories and cell walls. The deterioration of insulating materials and cell walls is undesirable as it results in increased thermal conductivity and, therefore, higher operating costs. The mineralogy of two dry-powder barriers was characterized by several methods. Results show that after 893 days in an aluminum reduction cell, corundum and wollastonite-based powder formed an incomplete calcium-fluoride barrier. This dry powder contained a vermiculite base. An anorthite-based powder was tested in a laboratory trial and formed a nepheline barrier with complete conversion of fluorine to stable mineralogical phases after 100 hours. Testing of this anorthite-based powder in aluminum-plant reduction cells is currently in progress.

INTRODUCTION

Barrier layers have been utilized for many years in the aluminum industry to protect insulating refractories from sodium fluoride and sodium aluminum fluoride penetration in Hall-Héroult reduction cells. These refractories have typically been dense, low-porosity firebricks.[1] In recent years, however, other refractories, such as low-cement castables[2] and dry powders, have been developed. The dry powders are typically composed of vermiculite and calcium-silicate, anorthite and gehlenite, or anorthite and additives. Anorthite-based dry powder barriers have been patented since 1984,[3] but have yet to be proven and accepted by the industry. Interest in dry powder is, in part, inspired by the idea that the high melting point of fluorite or nepheline would allow a solid impermeable barrier to form at operating conditions (950°C).

Although many studies have been conducted on dry powders, limited mineralogical results have been reported due to the complexities of these systems. X-ray diffraction (XRD) patterns are extremely complicated and difficult to interpret due to numerous overlapping peaks. The minerals associated with dry powders and reaction products have similar optical properties and atomic number composites, which make distinguishing between the various phases by reflected light microscopy (RLM), transmitted light microscopy (TLM), and scanning electron microscopy-back scattered imaging (SEM-BSI) difficult, if not impossible. These techniques, however, when used in collaboration with cathodoluminescence microscopy (CLM) and energy-dispersive spectroscopy (EDS) reveal intricate details of mineralogical reaction products not previously observed or reported.

CORUNDUM- AND WOLLASTONITE-BASED POWDERS

The corundum- and wollastonite-based dry powder was segmented into reacted bath material, hot face, interface, and cold face. Villiaumite (NaF) and corundum are the major phases in the reacted bath, with minor nepheline ($NaAlSiO_4$), beta-sodium-aluminate (β-$NaAl_{11}O_{17}$), and fluorite (CaF_2) phases present, as determined by XRD

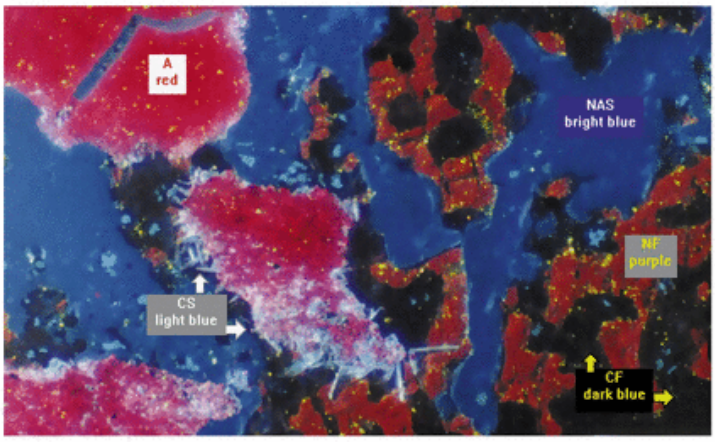

Figure 1. A CLM photomicrograph of a corundum- and wollastonite-based hot face zone of reacted dry powder. Unreacted sodium fluoride (dark purple, NF), corundum (red, A), and wollastonite prismatic crystals (light blue, CS) are dispersed between reaction products fluorite (dark blue, CL) and nepheline (bright blue, NAS) matrix.

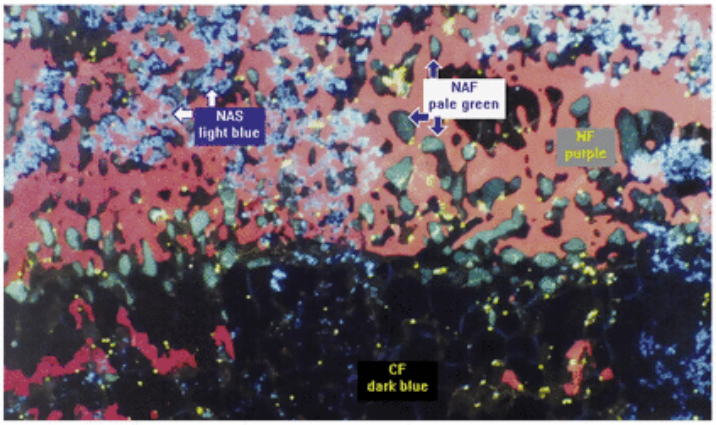

Figure 2. A CLM photomicrograph of the interface zone of corundum- and wollastonite-based reacted dry powder. The reaction product fluorite (dark blue, CF) forms a semibarrier to sodium fluoride (purple, NF) and cryolite (pale green, NAF). Fine-grained nepheline (light blue, NAS) is dispersed throughout.

(Table I). Trace amounts of wollastonite and nepheline are also present.

Major nepheline and lesser cryolite (Na_3AlF_6) phases are present at the hot face. Minor NaF and trace fluorite are also present, as well as unreacted corundum and wollastonite (Figure 1).

A wall of fluorite is present in the interface section between the hot face and the cold face (Figure 2). Although NaF is reduced at this fluorite barrier, it is still present beneath the barrier. Sodium fluoride in this area appears to have leached through the fluorite barrier. The fluorite zone is quite solid where it is present, but has patches of gaps that break up the barrier, making it ineffective to soluble NaF penetration.

Two phases are predominant in the cold face: fluorite and sodium fluoride. Fluorite and NaF each compose approximately 50 percent of the cold face section. In the interface zone, fluorite proved to be an inadequate barrier for NaF penetration into the cold face.

The studies show that a fluorite barrier was formed from the corundum and wollastonite-based dry powder. It was an incomplete barrier, however, after two and a half years in service. Cryolite was completely converted to solid crystalline phases of fluorite and nepheline, but significant sodium fluoride was present in the cold face of the reacted material.

Based on these results, the corundum- and wollastonite-based dry powder was only partially successful in converting fluorine into nonleachable forms. It is interesting that significant corundum and wollastonite are present in the hot face, indicating conditions were inadequate for complete reactions to take place. It is possible that the NaF penetrated too quickly for a reaction to occur, and that loose powder particles migrated into the bath prior to reaction and solidification of the melt.

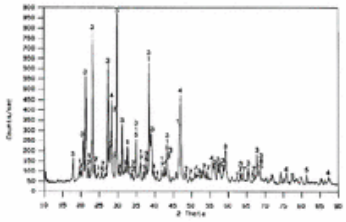

Figure 3. An x-ray diffraction pattern of the hot face of reacted anorthite-based dry powder showing major nepheline (3) and fluorite (4), and minor cryolite (1), anorthite (7), corundum (5), and NaF (2).

EXPERIMENTAL PROCEDURES AND MINERALOGICAL CHARACTERIZATION

Two dry powders were studied in this work: vermiculite ($(Mg,Fe,Al)_3(Al,Si)_4O_{10}(OH)_2{}^*4H_2O$), corundum ($Al_2O_3$), and wollastonite ($CaSiO_3$)-based powder from a cell autopsy and an anorthite ($CaAl_2Si_2O_8$)-based powder in a laboratory test. (The vermiculite, corundum, and wollastonite-based dry powder will be referred to as corundum and wollastonite-based.)

The corundum- and wollastonite-based dry powder was installed as a 75 mm layer placed on top of 100 mm vermiculite in a reduction cell at an aluminum plant. The powder was packed into place. After 893 days, the cell was autopsied, and reacted samples collected. These were sectioned for XRD, polished thin section analysis, and chemical analysis. The portion of reacted sample utilized for polished thin sectioning was impregnated with epoxy to retain its original orientation in the cell. Polished thin sections 27 mm × 46 mm × 30 µm thick were examined by RLM, TLM, SEM, and CLM. XRD samples were ground to –325 M, and chemical analysis samples were ground to –200 M. Leachable and nonleachable fluorine analyses were conducted. Difficulties with the analytical procedure yielded unreliable results; therefore, these results are not included in this article.

The anthorite-based powder was tested in the laboratory. Samples of 150 grams (43 mm depth) bath and 300 grams (56 mm depth) anorthite-based dry powder were heated in a 100 mm diameter graphite crucible at 950°C for 100 hours. The bath consisted of 70 percent cryolite and 30 percent NaF. After 100 hours, the crucible was cut in half and sectioned for XRD, polished thin section, and chemical analysis.

Mineralogical Characterization

The two dry powders were studied by XRD, RLM, TLM, SEM-BSI, EDS, and CLM. CLM was particularly useful, due to the brilliant luminescence of many of the minerals present. A Technosyn cold cathode luminescence model 8200 MKII cathodoluminescence attachment to a Nikon OPTIPHOT-POL optical microscope was utilized in this study, with operating conditions of 10–15 kV and 0.2–0.4 mA. Reacted dry powders are difficult to study mineralogically due to their similar optical properties, similar atomic number composites that are utilized by SEM-BSI, and complex XRD patterns. CLM is an electron microscopy technique in which the sample (polished thin sections, in this case) is bombarded with electrons. The energy difference between the excited and normal energy state of an electron in a trace element is emitted as a photon (visible light). Each mineral phase within a given sample usually contains the same trace elements. That mineral, therefore, luminesces the same color and intensity throughout that specific sample. Trace elements have the potential to act as luminescers, activators, quenchers, or nonluminescers. Crystal defects can also create luminescence within a mineral.

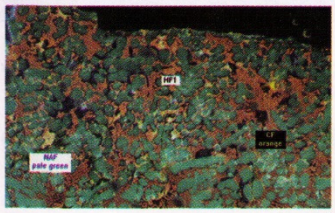

a 500 µm

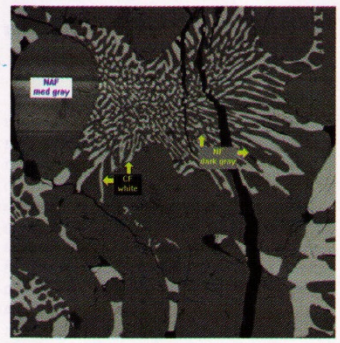

b 170 µm

Figure 4. Photomicrographs of HF1 in anorthite-based dry powder showing (a) cryolite (pale green, NAF) where elongated spheres are interspersed throughout a fluorite (orange, CF) and sodium fluoride (dark blue, NF) matrix as observed by CLM, and (b) a higher magnification of the eutectic fluorite (white) and NaF (dark gray) through SEM-BSI.

Table I. Corundum- and Wollastonite-Based Mineralogical Phases After 893 Days*

Section Location	Major Phases (>20%)	Minor Phases (10–20%)	Trace (<10%)
Reacted Bath	Villiaumite Corundum	Cryolite Diaoyudaoite Fluorite	Wollastonite Nepheline
Hot Face	Nepheline Cryolite	Villiaumite Corundum Wollastonite	Fluorite
Interface	Villiaumite Fluorite	Cryolite	Nepheline Wollastonite
Cold Face	Fluorite Villiaumite		

* Determined by XRD.

ANORTHITE-BASED POWDERS

In the laboratory test of the anorthite-based powder, approximately 75% of the original sample (bath combined with anorthite-based powder) remained after 100 hours at 950°C. The original depth of 99 mm decreased through compression and reaction to 74 mm. Approximately 65% of the sample is unreacted anorthite particles. The top half (hot face) and the bottom half (cold face) were ground for XRD. Nepheline and fluorite are the major XRD phases present in the hot face, with lesser cryolite, anorthite, corundum, and villiaumite (Figure 3). Anorthite is the only phase detected by XRD in the cold face (detection limit ~5%).

Transgressing from the hot face to the cold face, the anorthite-based dry powder segments are identified as hot face one (HF1) through hot face six (HF6), and cold face one (CF1) and cold face two (CF2). Table II outlines the minerals present in each of these segments as determined by RLM, TLM, SEM, and CLM.

Cryolite is a major constituent in the HF1 zone; it is present as 50–500 µm rounded grains dispersed uniformly throughout HF1 (Figure 4a). A few cryolite grains exhibit dendritic texture. Intermeshed between the cryolite grains are fluorite and NaF. The myrmekitic microstructure texture between fluorite and NaF (Figure 4b) is indicative of the eutectic relationship between these two phases. Faeroyvik has documented the solidus temperature for CaF_2 and NaF (in the presence of nepheline) on the pseudo-binary phase diagram of $2NaF\text{-}CaAl_2Si_2O_8$ as 800°C.[4] Very limited porosity is present in HF1.

Nepheline is the predominant phase in HF2, forming large (up to 2 mm) euhedral crystals (Figure 5). These large nepheline crystals grow significantly slower than the finer-grained nepheline crystals, which are at greater depth into the reacted dry powder. Between the large nepheline crystals, minor cryolite and fine-grained nepheline is present. HF3 is composed of fine-grained nepheline ranging in size from 25–150 µm, which grow (or react) at a much faster rate due to their relatively small size.

In addition to fine-grained nepheline interspersed with cryolite and minor fluorite, HF4 also contains a few corundum particles. The corundum particles are difficult to distinguish from nepheline and cryolite by SEM-BSI (Figure 6a), but are readily identified by CLM (Figure 6b). Corundum luminesces red, nepheline is bright blue,

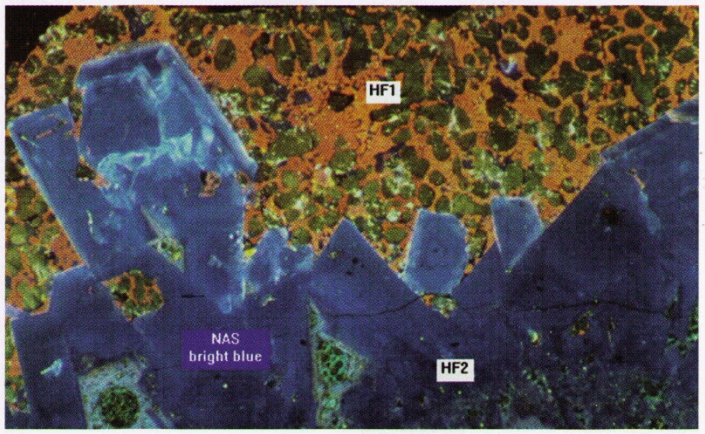

500 µm

Figure 5. A CLM photomicrograph of anorthite-based dry powder HF1 (top) and HF2 (bottom) showing a large crystalline nepheline (bright blue, NAS) barrier.

Table II. Anorthite-Based Mineralogical Phases and Depth of Sections After 100 Hours*

Location	Major (>20%)	Minor (<20%)	Depth (mm)	Characteristic
Hot Face 1	Cryolite Fluorite	Villiaumite	0–2.5	Eutectic fluorite-villiaumite
Hot Face 2	Nepheline	Cryolite	2.5–4.0	Large crystalline nepheline barrier
Hot Face 3	Nepheline Cryolite		4.0–7.0	Fine-grained nepheline
Hot Face 4	Nepheline Cryolite	Fluorite Villiaumite Fluorine-bearing nepheline Corundum	7.0–17.5	Fine-grained nepheline
Hot Face 5	Nepheline Fluorine-bearing nepheline	Fluorite Anorthite	17.5–21.0	Zoned nepheline
Hot Face 6	Anorthite	Nepheline	21.0–23.0	Anhedral nepheline
Cold Face 1	Anorthite	Nepheline Corundum	23.0–26.0	Anhedral nepheline
Cold Face 2	Anorthite	Nepheline	26.0–74.0	Anhedral nepheline

* Determined by RLM, TLM, SEM, and CLM.

and cryolite is pale blue (Figure 6b). Bulging in from the edge of the crucible at HF4 are textures identical to HF1: rounded grains of cryolite in a matrix of myrmekitic NaF and fluorite. This material, which extends 4.5 mm from the edge toward the center of the crucible, appears to have escaped the large nepheline crystalline barrier.

HF5 is the last zone to contain fluorine in any phase, either soluble or insoluble. Fine-grained nepheline is contained in a fluorine-bearing (<3% fluorine) nepheline matrix. Nepheline and fluorine-bearing nepheline ($NaAlSiO_4$ + 2–3 wt.% F) cannot be distinguished by SEM-EDS due to their very similar atomic number composites; however, fluorine-bearing nepheline luminesces red, and nonfluorine-bearing nepheline luminesces blue by CLM (Figure 7). An x-ray dot map of fluorine (Figure 8a) depicts 2–3 wt.% fluorine as blue and trace amounts of CaF_2 as green on the top half of the image, and essentially no fluorine (black) in the bottom half of the image. This is the same field of view as the image displayed in Figure 7. A calcium x-ray dot map of the same area shows anorthite as dull green (predominantly in the lower half of Figure 8b) and fluorite as bright green (trace amounts in the upper half of Figure 8b). It is not presently known if the fluorine in fluorine-bearing nephaline is leachable, but it is in very low

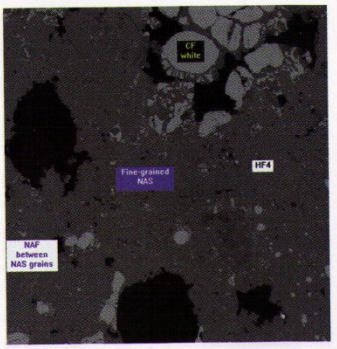

a

900 μm

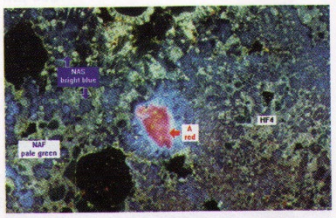

b

500 μm

Figure 6. Photomicrographs of anorthite-based dry powder at HF4 showing (a) how fluorite (white, CF) and porosity (black) are detectable by SEM-BSI, and (b) the same field of view by CLM showing fine-grained nepheline (bright blue, NAS), corundum (bright red , A), and fluorite (dark blue, CF) in a cryolite (pale green, NAF) matrix.

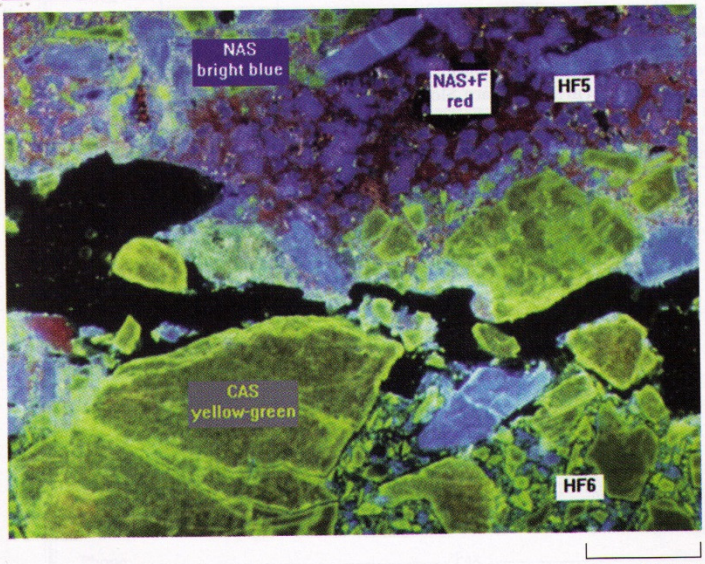

500 μm

Figure 7. A CLM photomicrograph of HF5 (top) and HF6 (bottom) in an anorthite-based dry powder. Fine-grained nepheline (bright blue, NAS) is zoned and contained in a fluorine-bearing nepheline (deep red, NAS + F) matrix. No fluorine phases exist beneath the red zone. Anorthite (CAS) luminesces yellow-green CL and is in powder form below the crack (black, CL).

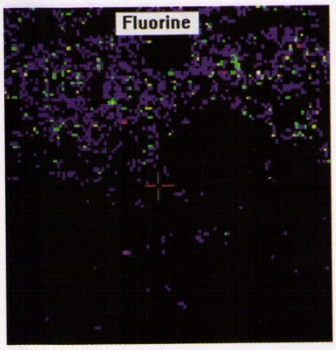

a 900 μm

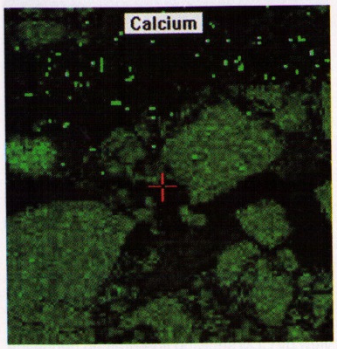

b 900 μm

Figure 8. SEM-EDS x-ray dot maps (same field of view as Figure 7) showing (a) fluorine and (b) calcium. Trace fluorine (<3 wt.%), predominantly in the upper half, is indicated as blue dots in (a). Anorthite, predominantly in the lower half, is represented as dull green dots in (b). Fluorite, sparsely scattered in the upper half, is represented as bright green dots in both. Essentially no fluorine in any form exists below the center of this field of view.

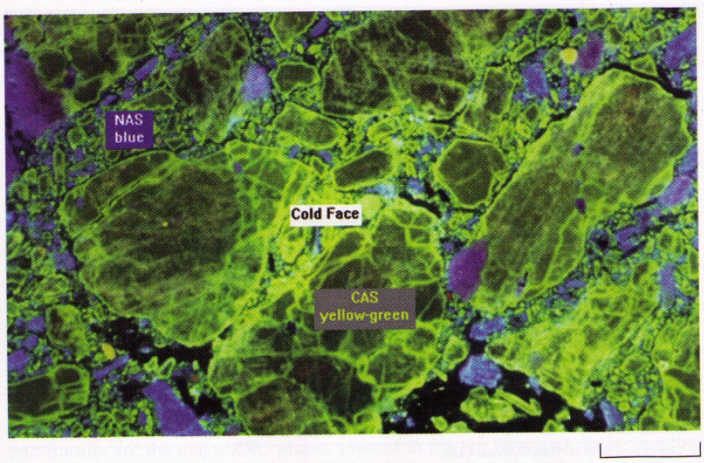

500 μm

Figure 9. A CLM photomicrograph of anorthite-based dry powder cold face showing predominant anorthite (yellow-green, CAS) and minor nepheline (bright blue, NAS) unconsolidated particles. No fluorine-bearing phases are present in the cold face sections.

concentrations (2–3 wt.%). Nonfluorine-bearing nepheline in this section is zoned, indicating more than one fluid deposition. Trace fluorite is present as small grains in HF5, and minor unreacted anorthite is also present.

Below the HF5 zone (toward the cold face), a crack in the dry powder extending through approximately one third the length of the polished thin section exists to a maximum thickness of 750 μm. This crack could be the result of outgassing. Regardless of the presence or absence of a crack, the material above this depth is solid material with limited porosity. The material below is powdered material. HF6 is powdered anorthite with a few of the smaller particles converted to nepheline (lower portion of Figure 7).

The cold-face zones are predominantly powdered anorthite with minor nepheline and trace corundum particles (Figure 9). XRD indicates only anorthite present (detection limit is approximately 5%).

The tests showed that a nepheline barrier was formed that covered most but not all of the length of the test crucible. In spite of the incomplete extent of the barrier, all of the cryolite and NaF at the reactant front were converted to solid crystalline phases of fluorite and nepheline. Fluorine-bearing nepheline is present in the hot face zones, but does not exist in the cold face. Slower growing nepheline (large crystals) is closer to the hot face, and faster growing nepheline (small crystals) is closer to the cold face. Fast growth near the cold face could be a function of NaF diffusing quickly through the dry powder to the center, not allowing for significant crystal growth. Zoned nepheline, which is also present toward the cold face, is most likely indicative of several periods of fluid exposure. The large nepheline crystals toward the top of the reacted dry powder, which are not zoned, are most likely in constant contact with bath materials and not exposed to separate fluid events. While performance of a material in a laboratory test is not as conclusive as an in-cell test, the anorthite-based powder shows promise as a barrier layer for reduction cells.

ACKNOWLEDGEMENT

The author thanks the Department of Geological Sciences at the University of Missouri at Columbia for making available to A.P. Green Industries their cathodoluminescence microscope during the course of this research.

References

1. A.T. Tabereaux, "Reviewing Advances in Cathode Refractory Materials," *JOM*, 44 (11) (1992), pp. 20–26.
2. C.T. Crozier, "Development of Comcast™-SCB-A High Alumina Low Cement Castable for Aluminium Reduction Cell Barrier Layers," *UNITECR '93 CONGRESS* (Sao Paulo, Brazil: 1993), pp. 862–871.
3. S.R. Brandtzaeg et al., "Experiences with Anorthite Powder-Based Penetration Barrier in 125 kA Soderberg Cell Cathodes," *Light Metals 1993* (Warrendale, PA: TMS, 1993), pp. 309–314.
4. M. Faeroyvik, "Chemical Reactions and Mineral Formation by Sodium Aluminium Fluoride Attack on Anorthite Based Refractories," Ph.D. thesis, University of Trondheim, Norway (1994).

ABOUT THE AUTHOR

Ann M. Hagni earned her Ph.D. in geology at the University of Missouri–Rolla in 1995. She is currently manager of applied mineralogy and analytical chemistry at A.P. Green Industries. Dr. Hagni is also a member of TMS.

For more information, contact A.M. Hagni, A.P. Green Industries, 1 Green Boulevard, Mexico, Missouri 65265; e-mail ahagni@compuserve.com.